Check for updates

ChemMedChem

Research Article
doi.org/10.1002/cmdc.202400232

Chemistry Europe
European Chemical Societies Publishing

www.chemmedchem.org

Microbubble-encapsulated Cobalt Nitrato Complexes for Ultrasound-triggerable Nitric Oxide Delivery

Patrick Koczera,*[a] Fabian Thomas,[b] Elena Rama,[a] Sven Thoröe-Boveleth,[c] Fabian Kiessling,[a] Twan Lammers,*[a] and Sonja Herres-Pawlis[b]

Cobalt complexes exhibit versatile reactivity with nitric oxide (NO), enabling their utilization in applications ranging from homogeneous catalysis to NO-based modulation of biological processes. However, the coordination geometry around the cobalt center is complex, the therapeutic window of NO is narrow, and controlled NO delivery is difficult. To better understand the complexation of cobalt with NO, we prepared four cobalt nitrato complexes and present a structure-property relationship for ultrasound-triggerable NO release. We hypothesized that modulation of the coordination geometry by ligand-modification would improve responsiveness to mechanical stimuli, like ultrasound. To enable eventual therapeutic testing, we here first demonstrate the in vitro tolerability of [Co(ethylenediamine)$_2$(NO)(NO$_3$)](NO$_3$) in A431 epidermoid carcinoma cells and J774A.1 murine macrophages, and we subsequently show successful encapsulation of the complex in poly(butyl cyanoacrylate) microbubbles. These hybrid Co-NO-containing microbubbles may in the future aid in ultrasound imaging-guided treatment of NO-responsive vascular pathologies.

Introduction

Nitric oxide (NO) is grouped among the gaseous signaling molecules and has captured interest in the research community due to its ability to modulate central biological processes like blood perfusion, inflammation or cell survival.[1] In addition to this, immune cells like granulocytes or macrophages leverage excess levels of NO for exploiting the antibacterial effects of reactive nitrogen species. In the body, production of NO is mediated by the enzyme group of nitric oxide synthetases (NOS) via the degradation of the amino acid arginine, or by reduction of nitrite/nitrate during the entero-salivary circulation.[2] Generation of NO by NOS is controlled by localized expression of different NOS isoforms, as the constitutively expressed neuronal and endothelial NOS balance NO levels for modulation of blood perfusion and neuronal activity. The inducible NOS of inflammatory cells produces excess levels of NO for antibacterial activity and immunomodulation.[3]

Due to this biological role, exogenous administration of NO via inhalation or via NO releasing molecules is clinical routine for treatment of e.g., pulmonal hypertension or ischemic heart disease. NO releasing molecules are utilized as "prodrugs", which release the active ingredient NO.[4] Besides nitroglycerin, the complex sodium nitroprusside, Na$_2$[Fe(CN)$_5$NO], is probably the most prominent example, for which the gas NO is complexed with iron and cyanide.[5] However, the drugs do not enable the local and temporal control of NO levels as compared to the tightly controlled biological balance. In addition, use as compressed gas for inhalation is limited by concerns regarding safety and applicability.[6]

This problem could be overcome by chemical modulation of the metal complexes to tailor properties, such as responsiveness to stimuli, e.g. by mechanical forces for triggered release mechanisms. Cobalt complexes exhibit versatile reactivity with NO and coordination of NO to cobalt centers influences its redox chemistry.[7] Ligand substitution dynamics govern the binding affinity of cobalt for NO. The electronic structure of the ligands modulates NO activation mechanisms as cobalt's d-orbitals facilitate π-backbonding with NO. Altering the ligand environment around the cobalt center can change the electronic structure and steric properties, thereby affecting the complex's affinity for NO. Additionally, adjusting conditions such as temperature, pressure, and solvent can influence the kinetics and thermodynamics of NO binding to cobalt. Moreover, the introduction of external stimuli such as light, electric fields, or other chemical agents can trigger reversible changes in the reactivity of the cobalt complexes.[8] Hence, cobalt complexes offer a possibility for triggered release of NO.

Microbubbles (MB) used for contrast-enhanced ultrasound imaging have recently been explored for triggered delivery of medical gases like O_2, NO, CO, Xe and H_2S, for use in cardio/neuro-protection and in models of myocardial infarction, and for enhancing drug delivery to pancreatic tumors and breast.[9]

[a] P. Koczera, E. Rama, F. Kiessling, T. Lammers
Institute for Experimental Molecular Imaging, Medical Faculty, RWTH Aachen University, Aachen, Germany
E-mail: pkoczera@ukaachen.de
tlammers@ukaachen.de

[b] F. Thomas, S. Herres-Pawlis
Institute of Inorganic Chemistry, RWTH Aachen University, Aachen, Germany

[c] S. Thoröe-Boveleth
Institute for Occupational, Social and Environmental Medicine, Medical Faculty, RWTH Aachen University, Aachen, Germany

Supporting information for this article is available on the WWW under https://doi.org/10.1002/cmdc.202400232

© 2024 The Author(s). ChemMedChem published by Wiley-VCH GmbH. This is an open access article under the terms of the Creative Commons Attribution Non-Commercial License, which permits use, distribution and reproduction in any medium, provided the original work is properly cited and is not used for commercial purposes.

© 2024 The Author(s). ChemMedChem published by Wiley-VCH GmbH

18607187, 0, Downloaded from https://chemistry-europe.onlinelibrary.wiley.com/doi/10.1002/cmdc.202400232 by Rwth Aachen Hochschulbibliothek, Wiley Online Library on [29/07/2024]. See the Terms and Conditions (https://onlinelibrary.wiley.com/terms-and-conditions) on Wiley Online Library for rules of use; OA articles are governed by the applicable Creative Commons License

The MB consist of a gas core, which is responsible for the detectable echo in ultrasound imaging, and a stabilizing shell, creating spheres in the size range of 1–10 μm. Different shell materials like phospholipids, polymers or proteins were developed in order to improve stability and increase circulation time.[10] Among these polymers poly(butyl cyanoacrylate) (PBCA) excels with biocompatibility and drug-loading, as the thick shell enables efficient encapsulation of drug molecules. Drug-loaded MB exposed to ultrasound waves give rise to different mechanical phenomena, namely stable or inertial cavitation, microstreaming and jet formation in combination with drug release. This leads ultimately to the permeation of biological barriers (referred to as sonopermeation) and ultrasound-mediated drug delivery.[11]

To explore the responsiveness of cobalt- and NO-containing complexes to ultrasound, we evaluated four previously developed cobalt complexes for NO release. After identification of one complex capable of ultrasound-induced NO release and in preparation for therapeutic evaluation we explored its biological tolerability and feasibility for encapsulation in ultrasound responsive MB with the shell composed of PBCA.

Results and Discussion

Cobalt nitrato complexes show potential for controlled release of NO. To investigate the release of NO, we synthesized four candidates exhibiting a low-spin d^8 Co^{I}-NO^{+} couple and differing in their ligands. In short, cobalt (−II) salts were dissolved in acetonitrile and purged with N_2 using standard Schlenk techniques. The corresponding ligands were added to the solution and N_2 was replaced by NO_2-free NO. It was previously described that N_2 or argon purge can release NO from the complex in solution, which is indicated specifically by colour change. Therefore, we re-examined this observation and explored the effect of mechanical triggering with ultrasound. Table 1 shows the results of the evaluation of NO release in addition to structural parameters of the evaluated complexes as described before.[12]

Sonication of the crystals did not induce any changes, and sonication of complexes in situ and after solvation in methanol also showed no impact on the complexes, except for [Co(ethylenediamine)$_2$(NO)(NO$_3$)](NO$_3$). For this complex, sonification in situ or after solvation in methanol induced a colour change from dark red-brown to pale-red, accompanied by a light white/pink precipitate (Figure 1). Quantification of absorbance before and after sonication revealed a prominent decline between 350 and 410 nm and between 410 and 600 nm. The most prominent decline of absorbance in the visible range was at 496 nm (Figure S1). This colour change is specific to the release of NO, as previously described for releasing NO by argon purge.[12a] Besides this, also changes in complexation by ligand exchange with e.g. water or OH^{-}, or in the oxidation state of cobalt, could explain the observed colour change.

As ultrasound-induced NO release was not described before, we evaluated the available structural information of the complexes for understanding the response. Notably, [Co(en)$_2$(NO)(NO$_3$)](NO$_3$) stands out due to its longest distance of cobalt to nitrogen (1.820 Å). Longer cobalt to nitrogen distances seem to indicate weaker bond strength, for which energy

Table 1. NO release properties and structural information of the evaluated complexes. [Co(en)$_2$(NO)(NO$_3$)](NO$_3$) has the longest Cobalt-to-NO-nitrogen bond, and a rather trigonal-bipyramid to vacant-octahedron coordination sphere, as compared to the more square-pyramid sphere of the other complexes. 2-aepyrr = N-(2-aminoethyl)pyrrolidine, fpin = perfluoropinacolate(2−), 2-aemor = N-(2-aminoethyl)morpholine, dmen = N,N-dimethyl-ethylenediamine, en = ethylenediamine.

Complex	[Co(2-aepyrr)(fpin)(NO)]	[Co(2-aemor)(fpin)(NO)]	[Co(dmen)(fpin)(NO)]	[Co(en)$_2$(NO)(NO$_3$)](NO$_3$)
NO-release by Argon	–	slow	–	–
NO-release by Ultrasound	–	–	–	yes
N–O [Å]	1.176(3)	1.169(3)	1.165(4)	1.173(3)
Co–N [Å]	1.787(2)	1.788(2)	1.799(3)	1.820(3)
Co–N–O [°]	123.8(2)	125.1(2)	126.6(3)	121.3(2)
S TBPY-5	3.5	3.7	5.6	7.7
S SPY-5	1.5	1.0	0.8	1.9
EOS(Co) EOS(NO)	+1	+1	+1	+1
EFO σ/π1	0.434	0.433	0.431	0.473
EFO π/π2	0.246	0.247	0.259	0.204

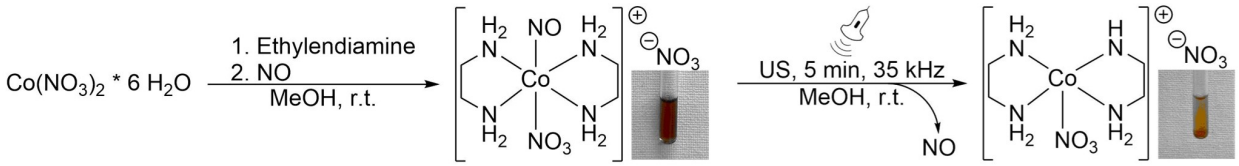


Figure 1. Four previously described cobalt nitrato complexes were successfully resynthesized.[12a] Ultrasound-induced release of NO was detected for [Co(en)$_2$(NO)(NO$_3$)](NO$_3$) by colour change.

© 2024 The Author(s). ChemMedChem published by Wiley-VCH GmbH

deposition by ultrasound is sufficient for bond disruption. In addition, the shape of the coordination polyhedron of the central cobalt atom in the complex differs from coordination polyhedron shapes in other complexes. Based on their X-ray structure, the complexes can be positioned on the Alvarez's shape map for pentacoordinate species, which is used in evaluation of continuous shape measures.[12b] While the position of $[Co(en)_2(NO)(NO_3)](NO_3)$ on this map indicates a shape of a vacant octahedron, other complexes rather cluster around a position indicating shapes in the transition from a trigonal-bipyramid to a vacant octahedron via Berry pseudo-rotation. These characteristics indicate a structure-property relationship, in which a long cobalt-to-NO-nitrogen bond and a vacant octahedron shape of the coordination sphere favour ultrasound-induced NO release.

Based on our findings that $[Co(en)_2(NO)(NO_3)](NO_3)$ showed ultrasound-triggered release of NO, we aimed to assess its tolerability for potential in vivo applications. Although cobalt is a trace element and essential in form of cobalamines as coenzyme for methionine synthase and methylmalonyl-CoA mutase, the cobalt ion is typically trapped within a stable corrin ring and not readily released. Soil bacteria are the natural source of cobalamines, and humans rely on its intake by animal or fortified foods.[13] Exogenous administration of cobalt has been shown to exhibit toxicity similar to other transition metals, impacting multiple organ systems and leading to conditions such as cardiomyopathy, interstitial lung disease and hearing loss. Pathophysiologically, Co^{2+} competes with Ca^{2+} and Mg^{2+} ions, disrupting cellular homeostasis and inhibiting enzymes involved in protein and RNA synthesis.[14] To evaluate the tolerability of $[Co(en)_2(NO)(NO_3)](NO_3)$, we incubated J774A.1 and A431 cells with various concentrations of the compound and assessed toxicity using LDH release and XTT testing as indicators of cell death via membrane permeation and metabolic disruption. Our study focused on A431 as robust neoplastic human epidermoid carcinoma cell line, which exhibits high proliferation, and the macrophage-derived J774A.1 cell line, which as inflammatory cell line can modulate inflammation by NO production. The results, depicted in Figure 2, showed no observable toxic effects at concentrations ranging from 0.1 to 100 μM, defined by cellular metabolism remaining above 80% of controls and cytotoxicity below 15%. Exemplary images of the in vitro viability analyses are provided in Figure S2. Statistical evaluation of the obtained results did not indicate significant differences between the evaluated complex concentrations and cell types (Figure 2).

Our next step involved the synthesis and assessment of MB loaded with $[Co(en)_2(NO)(NO_3)](NO_3)$ for contrast enhancement in ultrasound imaging. MB are commonly used as contrast agent for ultrasound imaging. Moreover, polymeric MB with PBCA as shell material show potential as drug carriers. Their thicker shell, ranging from 100–200 nm, allows for better encapsulation of drug molecules compared to standard phospholipid MB with a thinner shell of 1–4 nm.[15] MB respond to ultrasound by oscillation. By incorporating $[Co(en)_2(NO)(NO_3)](NO_3)$ into the MB shell, we aimed to enhance its interaction with ultrasound waves. The embedded complex within the shell would experience mechanical strain during oscillation, leading to MB destruction and cavitation.

Polymerization of the shell for MB synthesis was achieved through anionic emulsion polymerization in the presence of OH^- ions.[15a] $[Co(en)_2(NO)(NO_3)](NO_3)$ was added during polymerization alongside the monomer BCA for encapsulation in the MB shell. Mechanical agitation resulted in an air-in-water solution where polymerization of butyl cyanoacrylate (BCA) occurred at the interphase, yielding an encapsulated gas core surrounded by a polymeric shell (Figure 2A). We labeled these newly synthesized complex-loaded microbubbles as "NO Co MB". The size distribution of particles is depicted in Figure 3B, showing narrow size distribution between 1.43 μm to 2.43 μm peaking at 1.93 μm for the NO Co MB. In comparison to unloaded MB (mean diameter of 2.30 ± 0.62 μm), complex incorporation had no relevant effect on size distribution within the favorable range of 1–10 μm, which is a crucial factor regarding response to ultrasound and intravascular distribution after injection.[10]

To quantify the loading of NO Co MB with the cobalt complex, we assessed cobalt content via Inductively Coupled

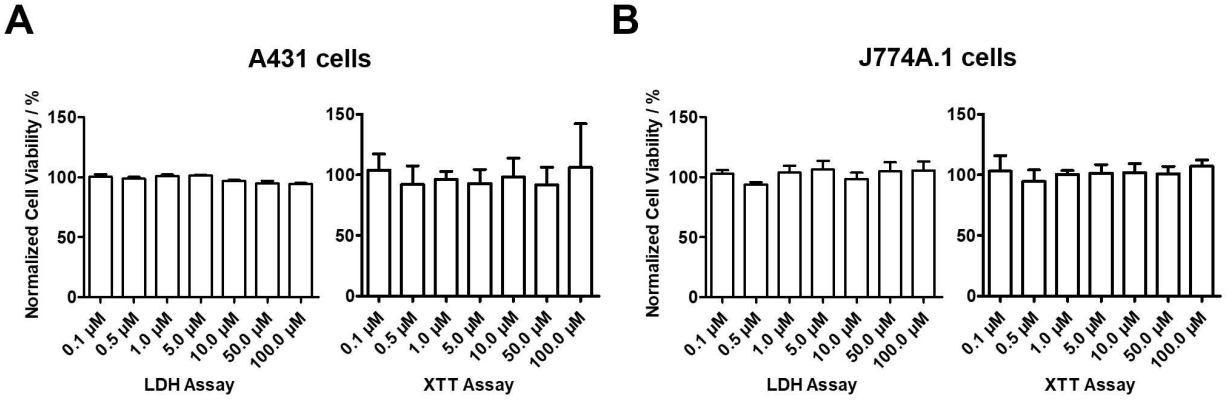


Figure 2. Toxicological evaluation of $[Co(en)_2(NO)(NO_3)](NO_3)$ in vitro. A431-epidermoid carcinoma cells (A) and J774A.1 murine macrophages (B) were treated with the complex and assessed for toxicity by LDH release and XTT testing, which indicate membrane permeation and metabolic disruption. The results are normalized to control conditions. Values represent mean ± SD, n = 3. No significant differences were detected comparing cell types and complex concentrations by two-way ANOVA.

© 2024 The Author(s). ChemMedChem published by Wiley-VCH GmbH

18607187, 0, Downloaded from https://chemistry-europe.onlinelibrary.wiley.com/doi/10.1002/cmdc.202400232 by Rwth Aachen Hochschulbibliothek, Wiley Online Library on [29/07/2024]. See the Terms and Conditions (https://onlinelibrary.wiley.com/terms-and-conditions) on Wiley Online Library for rules of use; OA articles are governed by the applicable Creative Commons License

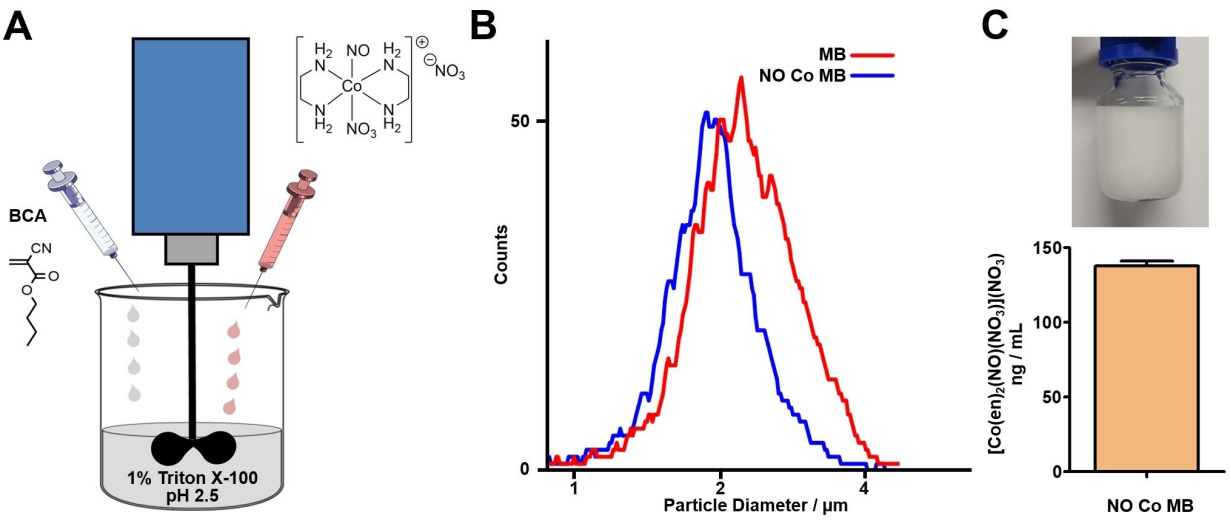


Figure 3. Synthesis of $[Co(en)_2(NO)(NO_3)](NO_3)$-loaded PBCA microbubbles (NO Co MB). (A) One-step synthesis of loaded MB was achieved by co-emulsifying an aqueous solution of n-butyl-cyanoacrylate (BCA) and the complex with 1% Triton X at pH 2.5 at 10 000 RPM for 1 hour, yielding an off-white emulsion with a final concentration of 6.8×10^8 NO Co MB/mL. (B,C) NO Co MB had a mean diameter of 1.93 (±0.50) µm containing 0.14 (±0.003) $[Co(en)_2(NO)(NO_3)](NO_3)$ µg/mL. Values represent mean ± SD, n = 3.

Plasma–Mass Spectrometry (ICP-MS) analysis. Successful loading was evidenced by a complex concentration of 0.14 (± 0.003) µg/mL derived from cobalt content at a MB concentration of 6.8×10^8 MB /mL (Figure 3C). Besides encapsulation within the polymeric shell of the MB, a fraction of the charged complex could also be adhering to the shell surface due to static interactions. In comparison to the concentration of metal carbonyl complexes in PBCA MB, the concentration of encapsulated $[Co(en)_2(NO)(NO_3)](NO_3)$ was low and could be explained by the rather hydrophilic character of the cobalt complex. Nonetheless, the concentration of encapsulated complex aligns with previous drug loading studies.[16,15b] The structure-property relationship we discussed earlier could be used to tailor the ligands in complexes, not just to enhance release characteristics, but also to improve encapsulation in PBCA MB.

To evaluate whether the NO Co MB could be detected by contrast-enhanced ultrasound imaging, we prepared in vitro gelatin phantoms. A clear contrast enhancement was demonstrated. In comparison to background levels without MB, NO Co MB enhanced the signal intensity in nonlinear contrast mode significantly, by a factor of 279 (±74), which was also the case for unloaded MB (by a factor of 224±85). No relevant differences in backscatter signals upon inverted nonlinear ultrasound pulses were detected comparing complex-loaded and standard unloaded MB. After application of a high intensity ultrasound sequence, nonlinear signal intensity decreased to background levels without MB, confirming MB fragmentation (Figure 4). In MB, backscatter signals depend on different factors like size, shell thickness, gas core and drug encapsulation. NO Co MB did not exhibit inferior performance compared to standard PBCA MB.[17] In fact, both formulations were equally fragmented by high-intensity ultrasound pulses, indicating feasibility for sonopermeation to enhance drug delivery. These results suggest that $[Co(en)_2(NO)(NO_3)](NO_3)$ did not negatively impact acoustic properties and that NO Co MB could be used for contrast enhancement in ultrasound imaging similarly to unloaded PBCA MB. However, higher encapsulation by tailored cobalt complexed could also affect the response of these loaded MB to incident ultrasound waves, therefore encapsulation of each new complex requires new evaluation of ultrasound responsiveness of the MB.

Taken together, we synthesized four previously described cobalt nitrato complexes, detected the ultrasound-induced release of NO from $[Co(en)_2(NO)(NO_3)](NO_3)$, and presented a structure-property relationship for the mechanochemical responsiveness of the NO-Co bond. Towards exploring therapeutic applications, we demonstrated tolerability of $[Co(en)_2(NO)(NO_3)](NO_3)$ in A431 human epidermoid carcinoma cells and J774A.1 immortalized murine macrophages, and showed successful encapsulating of the complex in PBCA MB, which we coined "NO Co MB".

The understanding of binding properties of ligands in cobalt nitrato complexes and confirmation of structure-property relationship helps to tailor ligand chemistry for controlling and manipulating the behavior of the cobalt-NO interaction. This approach not only offers opportunities for temporally and spatially improving NO release for biomedical applications, but also for tailoring the application of cobalt complexes in electrochemical sensing, as well as for catalysis in e.g. cross-coupling, hydrogenation and cycloaddition reactions.

While these results are encouraging, there are notable limitations to the current study that must be addressed. Primarily, the proposed structure-property relationship observed requires additional validation. A broader range of cobalt nitrato complexes should be investigated to substantiate these initial observations. NO release was here only verified qualitatively; a more precise and quantitative detection method would allow for a better comparison of how these complexes respond to ultrasound. For this purpose, a refinement in detection methodologies is needed, particularly for in vivo translational

© 2024 The Author(s). ChemMedChem published by Wiley-VCH GmbH

18607187, 0, Downloaded from https://chemistry-europe.onlinelibrary.wiley.com/doi/10.1002/cmdc.202400232 by Rwth Aachen Hochschulbibliothek, Wiley Online Library on [29/07/2024]. See the Terms and Conditions (https://onlinelibrary.wiley.com/terms-and-conditions) on Wiley Online Library for rules of use; OA articles are governed by the applicable Creative Commons License

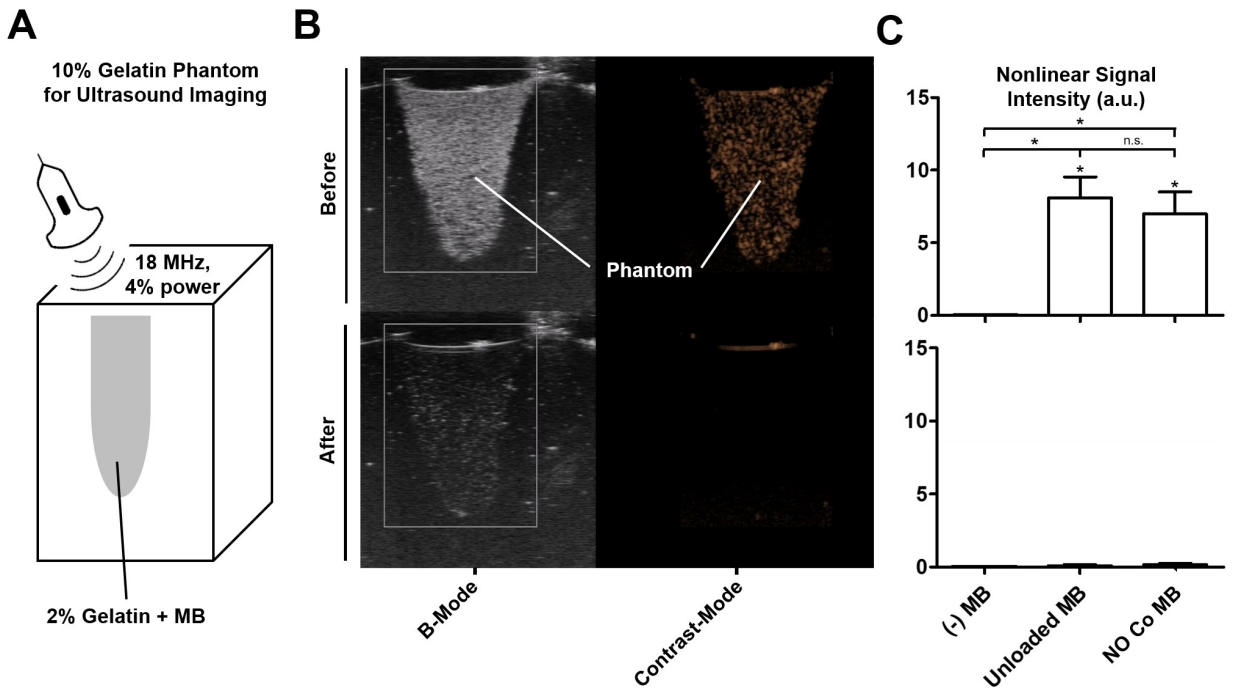


Figure 4. NO Co MB exhibited contrast enhancement in ultrasound imaging using B- and Contrast-mode. (A) Schematic illustration of the phantoms used for ultrasound imaging. (B) Contrast enhancement at 18 MHz was compared before and after ultrasound-mediated MB fragmentation in both B- and Contrast mode. (C) Quantification of MB-induced nonlinear signal enhancement in contrast mode showed no difference between NO Co MB and unloaded MB. Values represent mean ± SD, n = 3. *indicates $p < 0.0001$ and n.s. non-significance (i.e., $p > 0.05$), evaluated by two-way ANOVA and Tukey's multiple comparisons test.

research, where standard NO quantification techniques like the Griess reaction may cross-react with nitrites and nitrates present both within the cobalt complex $[Co(en)_2(NO)(NO_3)](NO_3)$ and in various biological fluids. Future studies could address this issue by implementing needle electrodes for electrochemical NO detection, or by employing electron paramagnetic resonance spectroscopy.

In terms of biocompatibility, our in vitro analysis demonstrated good tolerance by J774A.1 and A431 cell lines, yet these preliminary findings need further verification. Testing with primary cells from different organs, organoids, as well as systemic toxicity studies in rodent models would provide a more comprehensive understanding essential for moving towards translational applications. For eventual clinical translation, an ideal complex would exhibit non-toxicity while maintaining a delicate balance: it should be responsive enough to ultrasound-triggered NO release without being disrupted by the conditions within the body, such as reductive and oxidative environments, or unintended ligand exchange with halide ions, water molecules, hydroxide ions, or amino acids. Encapsulation within MB could offer a solution by confining the complex within the MB shell, thereby minimizing interactions with biological fluids, and allowing NO with its low molecular weight to diffuse rapidly into tissues following ultrasound-induced release.

Given NO's pivotal role in modulating tissue perfusion through vasodilation, future research should furthermore also focus on validating image-guided ultrasound-facilitated NO delivery therapies both in vitro and in vivo. For vascular pathologies characterized by constricted vessels leading to diminished organ perfusion and function, initial investigations might utilize endothelial cell cultures to monitor increases in intracellular cyclic guanosine monophosphate (cGMP), a key mediator in NO-driven smooth muscle relaxation and consequent vasodilation. Subsequent steps could include studying vessel dilation in explanted rat or mouse arteries perfused with complex-loaded MB for contrast-enhanced ultrasound-imaging and ultrasound-triggered NO release. Final preclinical validation could come from utilizing a rodent stroke model emblematic of the vessel narrowing seen post-subarachnoid hemorrhage. In such setups, ultrasound imaging could facilitate both detection of constricted vessels and localized NO release from complex-loaded MB, with the latter pharmacologically alleviating tissue hypoxia and damage in-situ, and thereby contributing to enhanced neural cell survival and brain function.

Methods

Synthesis and Characterization of the Cobalt Nitrato Complexes

The synthesis of the cobalt nitrato complexes was performed according to the protocol of previously reported by Popp et al..[12a] For evaluation of ultrasound-induced release of NO, 1.5–3.5 mg of the four different complexes were mixed with 200 μL of methanol in tubes and placed into a sonication bath at 35 kHz. For 15 minutes qualitative assessment of changes was performed. Optical absorbance of $[Co(en)_2(NO)(NO_3)](NO_3)$

© 2024 The Author(s). ChemMedChem published by Wiley-VCH GmbH

18607187, 0, Downloaded from https://chemistry-europe.onlinelibrary.wiley.com/doi/10.1002/cmdc.202400232 by Rwth Aachen Hochschulbibliothek, Wiley Online Library on [29/07/2024]. See the Terms and Conditions (https://onlinelibrary.wiley.com/terms-and-conditions) on Wiley Online Library for rules of use; OA articles are governed by the applicable Creative Commons License

before and after sonication was measured using a Tecan Infinite 200 spectrophotometer (Tecan, Männedorf, Switzerland).

Cell Culture

The XTT assay and LDH release assay were used to evaluate cellular metabolic activity and toxicity as per manufacturer's protocol. Two different cell lines were evaluated: A431 epidermoid carcinoma cells were obtained from ATCC and J774A.1 murine macrophages from Sigma-Aldrich. Five thousand cells were seeded in 96-well plates for overnight attachment in RPMI (A431 cells) or low-glucose DMEM (J774A.1 cells) supplemented with 10% fetal bovine serum (v/v) and 1% (v/v) penicillin/streptomycin maintained at 37 °C with 95% air and 5% CO_2. After overnight attachment, cells were incubated with fresh medium containing different concentrations of [Co-(ethylenediamine)$_2$(NO)(NO$_3$)]NO$_3$ (0.1, 0.5, 1, 5, 10, 50 and 100 μM) in aqueous DMSO (2% (v/v)). Cells were incubated for 4 hours. The colorimetric assays were quantitatively measured using the Tecan spectrophotometer.

Microbubble Synthesis

NO Co MB were synthesized based on a previously established 'one-step' loading protocol.[15a] 200 mg of [Co-(en)$_2$(NO)(NO$_3$)](NO$_3$) was dissolved in DMSO (4 mL) and added dropwise to aqueous solution (300 mL) of BCA and Triton-X (1% (v/v)) at pH 2.5. An Ultra-Turrax T-50 basic (IKA Werke, Germany) was used for agitation and the resulting mixture was emulsified at 10 000 RPM for 1 hour at room temperature. Residual [Co(en)$_2$(NO)(NO$_3$)](NO$_3$), DMSO and polymer fragments were centrifuged at 500 RPM for 20 minutes and the MB were washed 3 times with aqueous Triton-X (0.02% (v/v)) at pH = 7. Similarly, standard unloaded PBCA MB were synthesized without [Co(en)$_2$(NO)(NO$_3$)](NO$_3$). The MB formulations were stored in aqueous Triton-X (0.02% (v/v)). Using a Multisizer-4 Coulter Counter (Beckman Coulter, Germany) MB size and concentration were measured. For this, 2 μL of MB solution were mixed with 20 mL of ISOTON® II (Beckman Coulter) and readings were obtained in triplicate.

Inductively Coupled Plasma – Mass Spectrometry (ICP-MS) Analysis

Approx. 200 mg of the samples were taken and weighed exactly into microwave pressure digestion vessels. In addition to 1 mL of internal standard (rhodium, 1 mg/L, Merck, Darmstadt, Germany as 10 mg/L), 2.5 mL of nitric acid (suprapure, Merck, Darmstadt, Germany), 2.5 mL of hydrochloric acid (suprapure, Merck, Darmstadt, Germany), 2.5 mL of hydrogen peroxide (suprapure, Merck, Darmstadt, Germany) and 2.5 mL of MilliQ water were added to the sample. The sample mixtures were then digested in the Ethos.lab microwave pressure digestion system (MLS GmbH, Leutkirch, Germany). For this, the samples were first heated to 210 °C within 45 minutes. This temperature was hold for 15 minutes and then cooled to room temperature, diluted 1 : 10 and measured on the ICP-MS (8900-QQQ, Agilent, Waldbronn, Germany).

Ultrasound Imaging

In vitro custom-made gelatin phantoms were used for investigation of contrast enhancement of MB in response to ultrasound. Both types of MB were mixed in aqueous gelatin (2% (w/v) in 4.5 mL) (final concentration = 30 MB/μL) and embedded in gelatin (10% (w/v)) to set overnight. Ultrasound imaging was performed in non-linear contrast mode at 18 MHz frequency and 4% power using the preclinical VEVO 3100 ultrasound system (Visualsonics) and a linear-array based MS-250 transducer. For this, a pre-defined imaging sequence of total 200 frames in both B-mode and nonlinear contrast-enhanced ultrasound mode was recorded. For the first 5 seconds, a cine loop at 4% power (low mechanical index) was acquired. Then a destructive pulse with 100% power (high mechanical index) was applied. To calculate nonlinear signal intensity three images per phantom were collected and three regions of interest per image were drawn. Signal intensity in nonlinear contrast mode before and after MB fragmentation was quantified.

Statistical Analysis

All samples were measured in triplicate (n = 3). Descriptive statistics were used for obtained results and data are presented as means ± SD. Normal distribution was evaluated with the Shapiro-Wilk normality test. For small sample sizes, normal distribution was assumed. For evaluation of cytotoxicity in cell culture, values were normalized to control conditions, i.e. medium without probe for cytotoxicity. Viability in cell culture and nonlinear signal intensity in contrast-enhanced ultrasound imaging were evaluated by two-way ANOVA (analysis of variance) and Tukey's multiple comparisons test. In cell culture differences between cell types and between concentrations were evaluated and in ultrasound imaging signal intensities of the MB formulations, and before and after ultrasound-mediated fragmentation were compared. Statistical significance was considered at $p < 0.05$. GraphPad Prism 10 by GraphPad Software was used for statistical testing. Image analysis was performed with Imalytics Preclinical 2.1 by Gremse-IT and Fiji.[18]

Acknowledgements

This work was funded by the European Research Council (ERC CoG 864121, Meta-Targeting), German Research Foundation (DFG: GRK 2375 (grant 331065168), SFB 1066, and LA2937/4-1) and the Federal Ministry of Education and Research (CLIMBING CROHN, 01EK2201A). Open Access funding was enabled and

© 2024 The Author(s). ChemMedChem published by Wiley-VCH GmbH

18607187, 0, Downloaded from https://chemistry-europe.onlinelibrary.wiley.com/doi/10.1002/cmdc.202400232 by Rwth Aachen Hochschulbibliothek, Wiley Online Library on [29/07/2024]. See the Terms and Conditions (https://onlinelibrary.wiley.com/terms-and-conditions) on Wiley Online Library for rules of use; OA articles are governed by the applicable Creative Commons License

organized by Projekt DEAL. Open Access funding enabled and organized by Projekt DEAL.

Conflict of Interests

The authors declare no conflict of interest.

Data Availability Statement

The data that support the findings of this study are available from the corresponding author upon reasonable request.

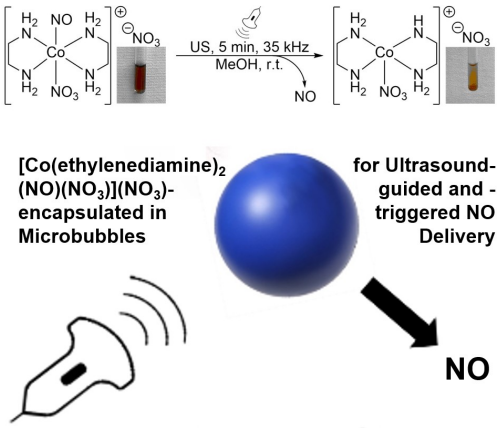
Keywords: Cobalt · Nitrogen oxides · Microbubbles · Ultrasound · Ultrasound imaging

[1] D. J. Polhemus, D. J. Lefer, *Circ. Res.* **2014**, *114*, 730–737.
[2] a) J. O. Lundberg, E. Weitzberg, M. T. Gladwin, *Nat. Rev. Drug Discovery* **2008**, *7*, 156–167; b) C. Farah, L. Y. M. Michel, J. L. Balligand, *Nat. Rev. Cardiol.* **2018**, *15*, 292–316.
[3] S. M. Andrabi, N. S. Sharma, A. Karan, S. M. S. Shahriar, B. Cordon, B. Ma, J. A. Xie, *Adv. Sci. (Weinheim, Ger.)* **2023**, *10*, e2303259.
[4] a) J. Kobayashi, I. Murata, *Ann. Intensive Care* **2020**, *10*, 61; b) L. J. Ignarro, C. Napoli, J. Loscalzo, *Circ. Res.* **2002**, *90*, 21–28.
[5] A. R. Butler, I. L. Megson, *Chem. Rev.* **2002**, *102*, 1155–1166.
[6] A. Odiba, C. Ukegbu, O. Anunobi, I. Chukwunonyelum, J. Esemonu, *Nanotechnol. Rev.* **2016**, *5*, 183–194.
[7] J. H. Enemark, R. D. Feltham, *Coord. Chem. Rev.* **1974**, *13*, 339–406.
[8] a) J. Pecak, W. Eder, B. Stöger, S. Realista, P. N. Martinho, M. J. Calhorda, W. Linert, K. Kirchner, *Organometallics* **2020**, *39*, 2594–2601; b) M. R. Walter, S. P. Dzul, A. V. Rodrigues, T. L. Stemmler, J. Telser, J. Conradie, A. Ghosh, T. C. Harrop, *J. Am. Chem. Soc.* **2016**, *138*, 12459–12471; c) H. Deka, S. Ghosh, S. Saha, K. Gogoi, B. Mondal, *Dalton Trans.* **2016**, *45*, 10979–10988; d) P. Kumar, Y. M. Lee, Y. J. Park, M. A. Siegler, K. D. Karlin, W. Nam, *J. Am. Chem. Soc.* **2015**, *137*, 4284–4287.
[9] a) S. Roovers, T. Segers, G. Lajoinie, J. Deprez, M. Versluis, S. C. De Smedt, I. Lentacker, *Langmuir* **2019**, *35*, 10173–10191; b) C. McEwan, J. Owen, E. Stride, C. Fowley, H. Nesbitt, D. Cochrane, C. C. Coussios, M. Borden, N. Nomikou, A. P. McHale, J. F. Callan, *J. Controlled Release* **2015**, *203*, 51–56; c) Q. G. Karwi, J. S. Bice, G. F. Baxter, *Basic Res. Cardiol.* **2017**, *113*, 6; d) H. Shekhar, A. Palaniappan, T. Peng, M. Lafond, M. R. Moody, K. J. Haworth, S. Huang, D. D. McPherson, C. K. Holland, *Neurotherapeutics* **2019**, *16*, 878–890; e) B. Theek, M. Baues, T. Ojha, D. Möckel, S. K. Veettil, J. Steitz, L. van Bloois, G. Storm, F. Kiessling, T. Lammers, *J. Controlled Release* **2016**, *231*, 77–85; f) G. Dimcevski, S. Kotopoulis, T. Bjånes, D. Hoem, J. Schjøtt, B. T. Gjertsen, M. Biermann, A. Molven, H. Sorbye, E. McCormack, M. Postema, O. H. J. Gilja, *J. Controlled Release* **2016**, *243*,172–181; g) A. Rix, M. Piepenbrock, B. Flege, S. von Stillfried, P. Koczera, T. Opacic, N. Simons, P. Boor, S. Thoröe-Boveleth, R. Deckers, J. N. May, T. Lammers, G. Schmitz, E. Stickeler, F. Kiessling, *Theranostics* **2021**, *11*, 9557–9570.
[10] P. Frinking, T. Segers, Y. Luan, F. Tranquart, *Ultrasound Med. Biol.* **2020**, *46*, 892–908.
[11] a) M. C. Cochran, J. Eisenbrey, R. O. Ouma, M. Soulen, M. A. Wheatley, *Int. J. Pharm.* **2011**, *414*, 161–170; b) S. Snipstad, E. Sulheim, C. de Lange Davies, C. Moonen, G. Storm, F. Kiessling, R. Schmid, T. Lammers, *Expert Opin. Drug Delivery* **2018**, *15*, 1249–1261.
[12] a) J. Popp, T. Riggenmann, D. Schröder, T. Ampßler, P. Salvador, P. Klüfers, *Inorg. Chem.* **2021**, *60*, 15980–15996; b) S. Alvarez, P. Alemany, D. Casanova, J. Cirera, M. Llunell, D. Avnir, *Coord. Chem. Rev.* **2005**, *249*, 1693–1708.
[13] a) R. Green, L. H. Allen, A. L. Bjørke-Monsen, A. Brito, J. L. Guéant, J. W. Miller, A. M. Molloy, E. Nexo, S. Stabler, B. H. Toh, P. M. Ueland, C. Yajnik, *Nat. Rev. Dis. Primers* **2017**, *3*, 17040; b) A. L. Bjørke-Monsen, V. Lysne, *Food Nutr. Res.* **2023**, *67*, 10.29219/fnr.v67.10257.
[14] D. G. Barceloux, *J. Toxicol. Clin. Toxicol.* **1999**, *37*, 201–206.
[15] a) P. Koczera, L. Appold, Y. Shi, M. Liu, A. Dasgupta, V. Pathak, T. Ojha, S. Fokong, Z. Wu, M. van Zandvoort, O. Iranzo, A. J. C. Kuehne, A. Pich, F. Kiessling, T. Lammers, *J. Controlled Release* **2017**, *259*, 128–135; b) M. Liu, A. Dasgupta, P. Koczera, S. Schipper, D. Rommel, Y. Shi, F. Kiessling, T. Lammers, *Mol. Pharm.* **2020**, *17*, 2840–2848; c) V. Paefgen, D. Doleschel, F. Kiessling, *Front. Pharmacol.* **2015**, *6*, 197; d) S. Fokong, B. Theek, Z. Wu, P. Koczera, L. Appold, S. Jorge, U. Resch-Genger, M. van Zandvoort, G. Storm, F. Kiessling, T. Lammers, *J. Controlled Release* **2012**, *163*, 75–81.
[16] V. Pathak, K. Roemhild, S. Schipper, N. Groß-Weege, T. Nolte, S. Ruetten, E. M. Buhl, A. El Shafei, M. Weiler, L. Martin, G. Marx, V. Schulz, F. Kiessling, T. Lammers, P. Koczera, *Small* **2022**, *18*, e2200924.
[17] a) L. J. Jablonowski, M. C. Cochran, J. R. Eisenbrey, N. T. Teraphongphom, M. A. Wheatley, *J. Biomed. Mater. Res. A.* **2017**, *105*, 3189–3196; b) T. B. Brismar, D. Grishenkov, B. Gustafsson, J. Härmark, A. Barrefelt, S. V. Kothapalli, S. Margheritelli, L. Oddo, K. Caidahl, H. Hebert, G. Paradossi, *Biomacromolecules* **2012**, *13*, 1390–1399; c) N. Teraphongphom, P. Chhour, J. R. Eisenbrey, P. C. Naha, W. R. Witschey, B. Opasanont, L. Jablonowski, D. P. Cormode, M. A. Wheatley, *Langmuir* **2015**, *31*, 11858–11867.
[18] a) J. Schindelin, I. Arganda-Carreras, E. Frise, V. Kaynig, M. Longair, T. Pietzsch, S. Preibisch, C. Rueden, S. Saalfeld, B. Schmid, J. Tinevez, D. White, V. Hartenstein, K. Eliceiri, P. Tomancak, A. Cardona, *Nat. Methods* **2012**, *9*, 676–682; b) F. Gremse, M. Stärk, J. Ehling, J. Menzel, T. Lammers, F. Kiessling, *Theranostics* **2016**, *6*, 328–341.

Manuscript received: March 30, 2024
Revised manuscript received: May 9, 2024
Accepted manuscript online: May 15, 2024
Version of record online: ■■, ■■

© 2024 The Author(s). ChemMedChem published by Wiley-VCH GmbH

18607187, 0, Downloaded from https://chemistry-europe.onlinelibrary.wiley.com/doi/10.1002/cmdc.202400232 by Rwth Aachen Hochschulbibliothek, Wiley Online Library on [29/07/2024]. See the Terms and Conditions (https://onlinelibrary.wiley.com/terms-and-conditions) on Wiley Online Library for rules of use; OA articles are governed by the applicable Creative Commons License



P. Koczera, F. Thomas, E. Rama, S. Thoröe-Boveleth, F. Kiessling, T. Lammers*, S. Herres-Pawlis*

1 – 8

Microbubble-encapsulated Cobalt Nitrato Complexes for Ultrasound-triggerable Nitric Oxide Delivery

Complexation of cobalt with nitric oxide (NO) is complex and its understanding offers applications in catalysis and biological processes. We evaluated four cobalt nitrato complexes for ultrasound-triggered release of NO. For future therapeutic evaluation we showed for one complex tolerability in vitro and encapsulation in polymeric microbubbles.

18607187, 0, Downloaded from https://chemistry-europe.onlinelibrary.wiley.com/doi/10.1002/cmdc.202400232 by Rwth Aachen Hochschulbibliothek, Wiley Online Library on [29/07/2024]. See the Terms and Conditions (https://onlinelibrary.wiley.com/terms-and-conditions) on Wiley Online Library for rules of use; OA articles are governed by the applicable Creative Commons License